$a\mu = 0$ gives the required expansion in each case. For $T$,

$$F(a,\mu) = \exp(-\mu c) \sum_{n=1}^{\infty} [(-a\mu)^{n-1}/(n+2)!] \times S_n(\omega_1, \omega_2, \omega_3),$$

and for $\overline{T}$,

$$F(a,\mu) = \exp(-\mu c)\{\tfrac{1}{6}cS_1(\omega_1,\omega_2,\omega_3) + a\sum_{n=2}^{\infty}[(-a\mu)^{n-2}/(n+2)!](-\mu c + n - 1) \times S_n(\omega_1,\omega_2,\omega_3)\}.$$

In these expressions, $S_n(\omega_1, \omega_2, \omega_3)$ is the fully symmetric function of order $n$ of three variables; *i.e.* $S_1 = \omega_1 + \omega_2 + \omega_3$, $S_2 = \omega_1^2 + \omega_2^2 + \omega_3^2 + \omega_1\omega_2 + \omega_3\omega_1 + \omega_2\omega_3$ *etc.* $S_n$ can be generated rapidly for any $n$ by using the simple algorithm $S_n = \omega_3 S_{n-1} + T_n$, $T_n = \omega_2 T_{n-1} + U_n$, $U_n = \omega_1 U_{n-1}$ with $S_0 = T_0 = U_0 = 1$.

### References


ALCOCK, N. W. (1970). *Crystallographic Computing*, edited by F. R. AHMED, pp. 271–278. Copenhagen: Munksgaard.
ALCOCK, N. W. (1974). *Acta Cryst.* **A30**, 332–335.
BLANC, E., SCHWARZENBACH, D. & FLACK, H. D. (1991). *J. Appl. Cryst.* **24**, 1035–1041.
BRAIBANTI, A. & TIRIPICCHIO, A. (1965). *Acta Cryst.* **19**, 99–103.
BUSING, W. R. & LEVY, H. (1957). *Acta Cryst.* **10**, 180–182.
CAHEN, D. & IBERS, J. A. (1972). *J. Appl. Cryst.* **5**, 298–299.
CLARK, R. C. (1993). *Acta Cryst.* **A49**, 692–697.
FLACK, H. D., VINCENT, M. G. & ALCOCK, N. W. (1980). *Acta Cryst.* **A36**, 682–686.
HOWELLS, R. G. (1950). *Acta Cryst.* **3**, 366–369.
*International Tables for X-ray Crystallography* (1959). Vol. II, pp. 291–305. Birmingham: Kynoch Press. (Present distributor Kluwer Academic Publishers, Dordrecht.)
MEULENAER, J. DE & TOMPA, H. (1965). *Acta Cryst.* **19**, 1014–1018.
REID, J. S. (1993). *Acta Cryst.* **A49**, 190–198.
SCHWARZENBACH, D. & FLACK, H. D. (1989). *J. Appl. Cryst.* **22**, 601–605.
SCHWARZENBACH, D. & FLACK, H. D. (1992). *J. Appl. Cryst.* **25**, 69.
ZACHARIASEN, W. H. (1967). *Acta Cryst.* **23**, 558–564.


*Acta Cryst.* (1995). **A51**, 897–902

# Rapid Suppression and Modulation of the Diffracted Beam in a Single Crystal Excited by Ultrasound

BY E. M. IOLIN

*Institute of Physical Energies of the Latvian Academy of Sciences*, 21 *Aizkraukles Street*, *Riga*, *LV*-1006, *Latvia*

(*Received* 13 *September* 1993; *accepted* 22 *May* 1995)


## Abstract

The results of a theoretical analysis of the influence of a high-frequency standing acoustic wave on the angular spectrum of a diffracted beam in a perfect crystal are presented. The rapid suppression and modulation of the intensity at the center of the diffraction pattern are found for the first time. The characteristic duration of this modulation is many times smaller than the period of the acoustic wave. These effects can be used for the suppression and modulation of a highly collimated monochromatic beam of synchrotron radiation.


## Introduction

The influence of the acoustic waves (AW) on the diffraction of X-rays and thermal neutrons in single crystals has been considered by many authors (*e.g.* Spencer & Pearman, 1970). Depending on the ultrasonic AW frequency, a distinction can be made between two different mechanisms. At $k_s \ll \Delta k_0$ ($\Delta k_0 = 2\pi/\tau$, $\tau$ is the extinction length, $k_s$ is the wave vector of the AW), the ultrasound deformations simply expand (in general) the Bragg-angle scattering interval [for a more detailed analysis see Kulda, Vrana & Mikula (1988), Lukas & Kulda (1989), Mikula, Lukas & Kulda (1992)]. A high-frequency ultrasonic AW with $k_s > \Delta k_0$ mixes the states corresponding to the different sheets of the dispersion surface (Köhler, Möhling & Peibst, 1974). Such a mixing leads to a number of effects, *e.g.* resonant suppression of the Borrmann effect (Entin, 1977), a new *Pendellösung* determined by AW (Iolin & Entin, 1983); Entin & Puchkova, 1984; Iolin, Zolotoyabko, Raitman, Kuvaldin & Gavrilov, 1986). In general, AW increases the integral intensity $I_h$ of the diffracted beam in perfect crystals and leads to decreasing $I_h$ in slightly deformed single crystals (Iolin, Raitman, Kuvaldin & Zolotoyabko, 1988).




ISSN 0108-7673 

Here, we report the results of a theoretical analysis of the high-frequency ultrasound influence on the angular spectrum of a diffracted beam in a perfect crystal for the Laue case (transmission geometry). It is well known that such a spectrum contains many peaks, which are phonon satellites. Köhler, Möhling & Peibst (1974) for the first time predicted and observed the decrease in intensity, $I_h(q)$, of the zeroth-order satellite (the main diffraction peak) due to AWs ($q$ is the impulse along the surface of the crystal; it is small near the center of the diffraction pattern). Their analysis is limited mainly by the case of moving (not standing) AWs. For a moving AW, the zeroth-order satellite shows no time dependence (at least for the case of a thick crystal) because the deformation picture in a moving AW is self-similar at different moments of time $t$.

We consider the decrease in intensity $I_h(q)$ of the zeroth-order satellite for the case of a *standing* AW in a perfect crystal. A strong time dependence of the diffracted-beam intensity $I_h(q)$ has been found in this case. For example, at some moment $t = t_1$, any deformation will be absent in the standing AW and the intensity $I_h(q)$ will be large near the center of the diffraction pattern. Suppose that, at the moment $t = t_0$, the standing AW amplitude $\mathbf{W} = \mathbf{W}_0$ and $I_h(0) \simeq 0$. At the next moment, $t = t_0 + \delta t$, $\mathbf{W} = \mathbf{W}_0 + \delta\mathbf{W}$, $|\delta\mathbf{W}| \ll |\mathbf{W}_0|$. A *coherent* addition of amplitudes of scattering between the layers of the crystal will be realized. Therefore, the intensity $I_h(0) \simeq (n\delta\mathbf{W})^2$ (the thickness of the crystal $T = n\lambda_s$, $\lambda_s$ is the wavelength of the AW) and it is rapidly increasing for the case of a thick ($n \gg 1$) crystal.

Therefore, the frequency of the *Pendellösung* movement is $n$ times higher than the frequency of the acoustic wave. We found that $I_h(q) \simeq q^4$ when $q \ll 1$ and $t = t_0$. Therefore, a rapid suppression of $I_h(q)$ may be observed in the central part of the main Laue diffraction peak for a very short time $\delta t$ (for example, at an AW frequency of 100 MHz, a suppression by a factor 1/50–1/100 will exist during 50–100 ps). The analysis of the steep time dependence of $I_h(q)$ for a standing AW is the main subject of this work. We have found that the transfer-matrix method is very useful for such a purpose. A very rapid intensity modulation of highly collimated monochromatic beams should be observed using synchrotron-radiation sources.

## Theory

We consider the symmetrical Laue diffraction in a single-crystal plate. The Takagi–Taupin equations then have the form

$$\begin{aligned} &-i\partial\Psi_0/\partial z - i\tan(\Theta_B)\partial\Psi_0/\partial x \\ &\quad + (\Delta k_0/2)\exp(i\mathbf{HU})\Psi_h = 0 \\ &-i\partial\Psi_h/\partial z + i\tan(\Theta_B)\partial\Psi_h/\partial x \\ &\quad + (\Delta k_0/2)\exp(-i\mathbf{HU})\Psi_0 = 0 \end{aligned} \tag{1}$$

$$\mathbf{U} = 4\mathbf{W}\cos(\omega_s t)\cos(k_s z), \quad \lambda_s = 2\pi/k_s, \quad \tau = 2\pi/\Delta k_0, \tag{2}$$

$$T = n\lambda_s, \quad n = 1, 2, \ldots . \tag{3}$$

$\Psi_0$, $\Psi_h$ are the amplitudes of incident and diffracted beams, $\Delta k_0$ is the gap between the sheets of the dispersion surface, $\tau$ is the extinction length, $\mathbf{H}$ is the diffraction vector, $x$, $z$ are the axes parallel and perpendicular to the plate surface, $T$ is the plate thickness, $\mathbf{U}$ is the displacement of a nucleus in the transversal AW with amplitude $\mathbf{W}$, angular frequency $\omega_s$ and wave vector $\mathbf{k}_s$. The standing transversal AW is excited between two surfaces of the single-crystal plate. We assume the boundary condition (3). Another important case $T = (2n+1)\lambda_s/2$ may also be considered but suppression of $I_h(q)$ is not so strong in this case. The moment $Q_x/\tan\Theta_B$ along the $x$ axis is conserved. Equations (1) can be transformed to the simpler and dimensionless form

$$\begin{aligned} &-2i\mathrm{d}\Phi_0/\mathrm{d}\xi + [\mathrm{d}(\mathbf{HU})/\mathrm{d}\xi]\Phi_0 + q\Psi_0 + p\Psi_h = 0 \\ &-2i\mathrm{d}\Phi_h/\mathrm{d}\xi - [\mathrm{d}(\mathbf{HU})/\mathrm{d}\xi]\Phi_h - q\Psi_h + p\Psi_0 = 0 \end{aligned} \tag{4}$$

$$\mathbf{HU} = 4\mathbf{HW}\cos(\omega_s t)\cos\xi, \quad p = \Delta k_0/k_s, \quad \xi = k_s z \tag{5}$$

$$\begin{aligned} Q_x &= k_s q/2\tan\Theta_B, \quad \delta\Theta = q\Delta\Theta_0/p, \\ \Delta\Theta_0 &= \Delta k_0/2k_0\sin\Theta_B, \quad \Theta = \Theta_B + \delta\Theta, \\ \Psi_0 &= \Phi_0\exp[i(\mathbf{HU} + q\xi)/2], \\ \Psi_h &= \Phi_h\exp[-i(\mathbf{HU} + q\xi)/2]. \end{aligned} \tag{6}$$

$p > 1$ and $p < 1$ correspond to the cases of low-frequency and high-frequency ultrasound, respectively, $\Theta_B$ is the Bragg angle, $\Theta$ is the angle between the incident beam and the surface normal to the plate and $2\Delta\Theta_0$ is the ordinary FWHM of the rocking curve.

We consider the role of the instantaneous deformation ($t = 0$). The coefficients of (4) are periodic functions of $x$. Therefore, it seems natural to use the transfer-matrix method for the analysis of (4). Suppose we know the solution of (4) in the interval $0 \le \xi \le 2\pi$. The solutions at $\xi = 2\pi$ and $\xi = 0$ are connected by the matrix $\mathbf{R}(1,0)$:

$$\begin{aligned} &\begin{pmatrix} \Phi_0 \\ \Phi_h \end{pmatrix}_{\xi=2\pi} = \mathbf{R}(1,0)\begin{pmatrix} \Phi_0 \\ \Phi_h \end{pmatrix}_{\xi=0}, \\ &\mathbf{R}(1,0) = \begin{pmatrix} R_{11} & R_{12} \\ R_{21} & R_{22} \end{pmatrix}, \quad \Phi \equiv \Phi_0, \Phi_h. \end{aligned} \tag{7}$$

The general expression for the unitary matrix $\mathbf{R}$ has the form (Landau & Lifshitz, 1965)

$$\mathbf{R}(1,0) = \exp[i\varphi + i(\mathbf{g}\boldsymbol{\sigma})/2]. \tag{8}$$

Here, $\varphi$, $g_{x,y,z}$ are numerical parameters of $\mathbf{R}(1,0)$; $\sigma_{x,y,z}$ are Pauli matrices. We will omit in the following the unimportant (for the calculation of $I_h$) phase $\varphi$. It is necessary to emphasize that we do not suppose that the scattered intensity is small in the region of $q > 1$. The solution $\Phi(\xi = 2\pi n)$ on the exit surface of the crystal is defined by the exact formula

$$\Phi(\xi = 2\pi n) = \exp[in(\mathbf{g}\boldsymbol{\sigma})/2]\Phi(\xi = 0). \tag{9}$$

The matrix $\exp[in(\mathbf{g}\boldsymbol{\sigma})/2]$ can be easily diagonalized using the well known relation

$$\exp[in(\mathbf{g}\boldsymbol{\sigma})/2] = \cos(ng/2) + i(\mathbf{g}\boldsymbol{\sigma})\sin(ng/2)/g. \tag{10}$$

Therefore, the intensity $I_h$ of the diffracted beam can be exactly calculated as

$$I_h = (1 - g_z^2/g^2)\sin^2(ng/2). \tag{11}$$

Expression (11) is excellently suited for the numerical calculation of $I_h$ for the case of a thick ($n \gg 1$) crystal. It is not necessary to find numerically a solution of the Takagi–Taupin (TT) equations (4) for such a thick crystal, it is enough to solve the TT equations for a thin crystal ($T = \lambda_s$) and then to find the parameters $\mathbf{g}$ and to apply (11). In order to analyze the parameters $\mathbf{g}$, we rearrange Takagi–Taupin equations (4) to the more suitable form

$$\begin{aligned}
&-i\mathrm{d}F_0/\mathrm{d}\xi + (p/2)\exp(i\mathbf{HU} + iq\xi)F_h = 0,\\
&-i\mathrm{d}F_h/\mathrm{d}\xi + (p/2)\exp(-i\mathbf{HU} - iq\xi) = 0,\\
&\qquad \Phi_0 = F_0\exp[-i(\mathbf{HU} + q\xi)/2],\\
&\qquad \Phi_h = F_h\exp[+i(\mathbf{HU} + q\xi)/2].
\end{aligned} \tag{12}$$

Solutions of (12) at $\xi = 2\pi$ and $\xi = 0$ are connected by the matrix $\mathbf{R}^f$:

$$\begin{aligned}
\mathbf{R}(1,0) = {}& \exp[-i\sigma_z/2(\mathbf{HU} + q\xi)|_{\xi=2\pi}]\\
&\times \mathbf{R}^f \exp[i\sigma_z/2(\mathbf{HU} + q\xi)|_{\xi=0}].
\end{aligned} \tag{13}$$

Consider the matrix $S(q)$ transforming the solution of Takagi–Taupin equations at $\xi = 0$ to that at $\xi = \pi$, that is at the distance $\lambda_s/2$. $S(q)$ is described in a form similar to (8). $\mathbf{R}^f$ and $S(q)$ are mutually related as

$$\begin{aligned}
\mathbf{R}^f(q) = {}& \begin{pmatrix} S_{11}^*(-q) & S_{21}^*(-q)\exp(i2\pi q) \\ S_{12}^*(-q)\exp(-i2\pi q) & S_{22}^*(-q) \end{pmatrix}^{-1}\\
&\times \begin{pmatrix} S_{11}(q) & S_{12}(q) \\ S_{21}(q) & S_{22}(q) \end{pmatrix}.
\end{aligned} \tag{14}$$

Let us suppose that we take such an instantaneous displacement $\mathbf{U} = \mathbf{U}_0$ or amplitude $\mathbf{W} = \mathbf{W}_0$ of the acoustic wave ($t = 0$) that the probability of scattering $P_{\lambda_s/2}(q)$ in the thin crystal with $T = \lambda_s/2$ is equal to zero at the center of the diffraction pattern, $P_{\lambda_s/2}(q = 0) = 0$. It is obvious from the symmetry of scattering and confirmed by results of the direct numerical solution of the Takagi–Taupin equations (see Fig. 1) that, at $q \ll 1$,

$$P_{\lambda_s/2} \simeq q^2. \tag{15}$$

Therefore, nondiagonal terms $S_{12} \simeq S_{21} \simeq q$. $S(q)$ is expressed in the linear approximation over $q$ and $\delta\mathbf{W}$ in the form

$$\begin{gathered}
S(q) \simeq 1 + iqA\boldsymbol{\sigma} + iB\boldsymbol{\sigma}\delta\mathbf{W}\\
\delta\mathbf{U} = \mathbf{U} - \mathbf{U}_0,\quad \delta\mathbf{W} = \mathbf{W} - \mathbf{W}_0,\quad A = A^*,\quad B = B^*.
\end{gathered} \tag{16}$$

$A$, $B$ are numerical constants. According to the optical theorem, the imaginary part of the amplitude of 'forward scattering' is proportional to the total cross section. The scattering at the crystal with $T = \lambda_s/2$ is absent at the center ($q = 0$) of the diffraction pattern. Therefore, $A_z = B_z = 0$. After simple calculations, we find

$$\mathbf{R}^f \simeq 1 + i2B\boldsymbol{\sigma}\delta\mathbf{W}. \tag{17}$$

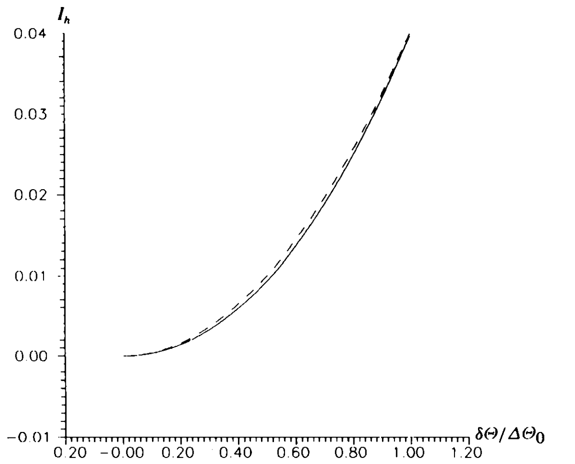


Fig. 1. Diffraction at the layer $T = \lambda_s/2 = 25\,\mu\mathrm{m}$; $\tau = 115\,\mu\mathrm{m}$; $\mathbf{HW} = 0.587$; —— numerical calculation; – – – $I_h = 0.04 \times (\delta\Theta/\Delta\Theta_0)^2$.

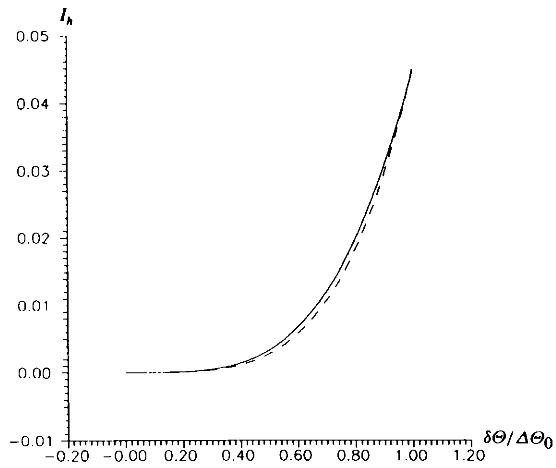


Fig. 2. Diffraction at the layer $T = \lambda_s = 50\,\mu\mathrm{m}$; $\tau = 115\,\mu\mathrm{m}$; $\mathbf{HW} = 0.587$; —— numerical calculation; – – – $I_h = 0.045 \times (\delta\Theta/\Delta\Theta_0)^4$.

Therefore, terms linear in $q$ are absent in the nondiagonal elements of $\mathbf{R}^f$; these elements are proportional to $q$ and $\delta\mathbf{W}$:

$$\mathbf{R}^f \simeq 1 + 2iB\sigma\delta\mathbf{W} + 2iC\sigma q^2, \quad C = C^*. \tag{18}$$

$C$ is a numerical constant. If $\delta\mathbf{W} = 0$, then the probability of scattering $P_{\lambda_s/2}(q)$ at the crystal thickness $T = \lambda_s$ is

$$P_{\lambda_s} \simeq q^4. \tag{19}$$

This result is also confirmed by the results of direct numerical solution of the Takagi–Taupin equations (see Fig. 2). Therefore, there exists not only weak scattering in each $\lambda_s/2$ layer but also almost complete compensation of the diffraction at one $\lambda_s/2$ layer owing to the diffraction at the neighboring $\lambda_s/2$ layer. After simple calculations, we find

$$\begin{aligned} g_z &\simeq -2\pi q, \\ g_\alpha &\simeq (4\delta\mathbf{W}B_\alpha + 4q^2C_\alpha)\exp(i\alpha\mathbf{HU}|_{\xi=0} + i\alpha\pi q), \\ &\alpha = \pm 1, \quad B_\alpha = B_x + i\alpha B_y, \\ &C_\alpha = C_x + i\alpha C_y, \\ I_h(q) &\simeq 16(\delta\mathbf{W}B + q^2C)^2/[(2\pi q)^2 \\ &+ 16(\delta\mathbf{W}B + q^2C)^2]\sin^2\{n/2[(2\pi q)^2 \\ &+ 16(\delta\mathbf{W}B + q^2C)^2]^{1/2}\}. \end{aligned} \tag{20}$$

### Analysis of results

Let us discuss the last term in $I_h(q)$ [(20)] when $\delta\mathbf{W} = 0$ and $q \ll 1$. This interference term leads to the disappearance of $I_h$ at the angle $\delta\Theta_A$:

$$\delta\Theta_A = \Delta\Theta_0\tau m/T, \tag{21}$$

where $m$ is an integer, $\tau$ is the extinction length, $T$ is the thickness of the crystal. Equation (21) is also confirmed by the results of numerical calculations (see Figs. 3 and 4). It is well known that the period of the ordinary *Pendellösung* is defined by the gap $\Delta k_0$ between the sheets of the dispersion surface. The scattering at the crystal thickness $T = \lambda_s$ is equal to zero or, more exactly, proportional to $q^4$ in our case. Therefore, the sheets of the dispersion surface (DS) are crossed with each other, the ordinary gap between them being absent when $\delta\mathbf{W} = 0$. Acoustic interference beats of $I_h$ [(20), (21)] are induced by transitions with the momentum $1/T$ between the sheets of the DS. $I_h(q)$ in (20) may be approximated by

$$\begin{aligned} I_h(q) &\simeq 16(\delta\mathbf{W}B + q^2C)^2/[(2\pi q)^2 + 16(\delta\mathbf{W}B)^2] \\ &\times \sin^2\{n/2[(2\pi q)^2 + 16(\delta\mathbf{W}B)^2]^{1/2}\}. \end{aligned} \tag{22}$$

Therefore, the gap $\Delta k_s$ between sheets of the DS is $\Delta k_s \simeq \delta\mathbf{W}$ and the corresponding characteristic length is large ($\tau_s = 2\pi/\Delta k_s \gg \tau$, $\tau_s = \pi\lambda_s/2/|\delta\mathbf{W}B|$, $\tau_s \gg \tau$).

We have studied the following examples: $\tau = 115\ \mu\text{m}$; $k_s/\Delta k_0 = 2.3$; $T = 500\ \mu\text{m}$ $(n = 10)$ and $1000\ \mu\text{m}$ $(n = 20)$. In order to find the numerical parameters $B$ and $C$, we compare the results of the direct numerical solution of the Takagi–Taupin equations and (20) when $T = 50\ \mu\text{m}$. We have found that

$$\begin{aligned} I_h(y) &\simeq G^2/[(2\pi\Delta k_0 y/k_s)^2 + G^2] \\ &\times \sin^2\{n/2[(2\pi\Delta k_0 y/k_s)^2 + G^2]^{1/2}\}, \end{aligned} \tag{23}$$

$$G^2 = G_{11}y^4 + G_{22}(\delta\mathbf{W})^2 + G_{12}y^2\delta\mathbf{W}, \quad y = \delta\Theta/\Delta\Theta_0,$$
$$G_{11} \simeq 0.35, \quad G_{22} \simeq 31.2, \quad G_{12} \simeq -0.4.$$

Formula (23) is in good agreement with the results of the numerical solution of the Takagi–Taupin equations. We have found above that diffraction is absent at the crystal thickness $T = \lambda_s$ when $q = 0$ and $\mathbf{W} = \mathbf{W}_0$. When

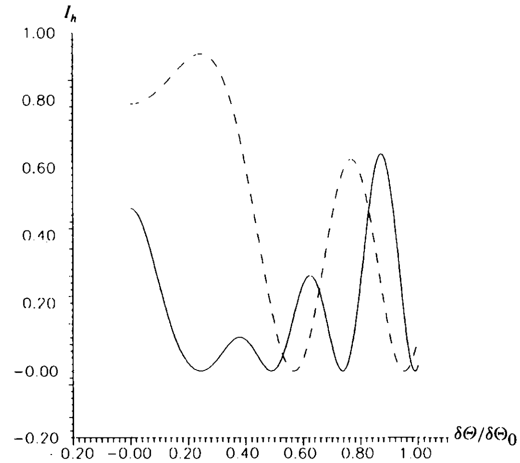


Fig. 3. Diffraction at the single-crystal plate. $T = 500\ \mu\text{m}$. – – – Ordinary *Pendellösung*; —— **HW** = 0.593 but the $I_h$ scale is increased 20 times; a very small gap between the sheets of the DS is present.

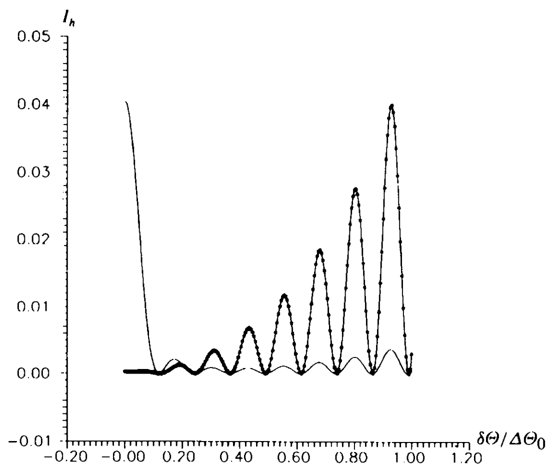


Fig. 4. The dependence of $I_h$ at the center of the diffraction pattern on the AW amplitude **W**. $T = 1000\ \mu\text{m}$. —— **HW** = 0.587; —•— **HW** = 0.6 but the $I_h$ scale is decreased 10 times.

$\mathbf{W} = \mathbf{W}_0 + \delta\mathbf{W}$, the amplitude of scattering $A_s(q = 0)$ at the crystal is

$$A_s(q = 0) \simeq n(\mathbf{H}\delta\mathbf{W}) \qquad (24)$$

and the intensity of the diffracted beam

$$I_h(q = 0) \simeq (n\mathbf{H}\delta\mathbf{W})^2. \qquad (25)$$

A coherent addition of amplitudes between $\lambda_s$ layers (25) leads to the strong dependence of the first peak in the *Pendellösung* on **HW**. This conclusion is confirmed by results of direct numerical calculations (see Fig. 4, $\lambda_s = 50$, $T = 1000\,\mu\text{m}$, $n = 20$).

The intensity at the center of the diffraction pattern is

$$I_h(q = 0) \simeq \sin^2(2n\delta\mathbf{W}B). \qquad (26)$$

Therefore, deep and rapid oscillations of the diffraction fringes will exist in the time region near $t = t_0$, $I_h(q = 0, t = t_0) = 0$. The characteristic frequency $\omega_p$ of these oscillations is $\sim n = T/\lambda_s \gg 1$ times higher than the frequency of the acoustic wave. In general, the whole picture of the *Pendellösung* (11) will oscillate with this large frequency $\omega_p \gg \omega_s$.

Let us introduce some values, *e.g.* $\mu_s$, the coefficient of the diffractional suppression by the acoustic wave,

$$\mu_s = J_{\mathbf{h}}(\mathbf{HW} = 0)/J_{\mathbf{h}}(\mathbf{HW}). \qquad (27)$$

$J_{\mathbf{h}}(\mathbf{HW})$ is the integral intensity of the diffracted beam in the angle interval $-\Delta\Theta_0 \le \delta\Theta \le \Delta\Theta_0$ [(6)], that is, within the ordinary FWHM rocking curve. We found values of $\mu_s$ to be large in all cases. We shall give an account of several results when the plate thickness $T = 500\,\mu\text{m}$. $\mu_s$ reaches a very large value (up to 74) and is extremely strongly dependent on the instantaneous displacement **U** in the acoustic wave (see Fig. 5). For example, $\mu_s = 74.6$ at $\mathbf{HW} = 0.5878$ and $\mu_s = 41$ at $\mathbf{HW} = 0.580$. Such a strong dependence of $\mu_s$ on **HW** can be explained by the first terms in (20), (22) and (23) being very sensitive to $\delta\mathbf{W}$, that is to the AW amplitude. It is interesting also that, in spite of the strong suppression of intensity $I_h(q)$ near the center of the rocking curve, the integral intensity $I_{hi}$ for all directions of the difracted beam is approximately twice as large as that for the perfect crystal without acoustic excitation (Fig. 6*a*). The large value of $\mu_s$ leads to the corresponding increase in the intensity of the forward-scattering beam. $\mu_s$ strongly depends on **HW**. For example, the decrease in $I_h$ of between 40 and 74 times will be in our case at $0.58 < \mathbf{HW} < 0.596$ (see Fig. 5). Therefore, for the ultrasound frequency 100 MHz, we shall have very short ($\sim$ 50–100 ps) intervals of the deep suppression of the diffracted-beam intensity. It is also very interesting to observe the strong and steep dependence on time of the

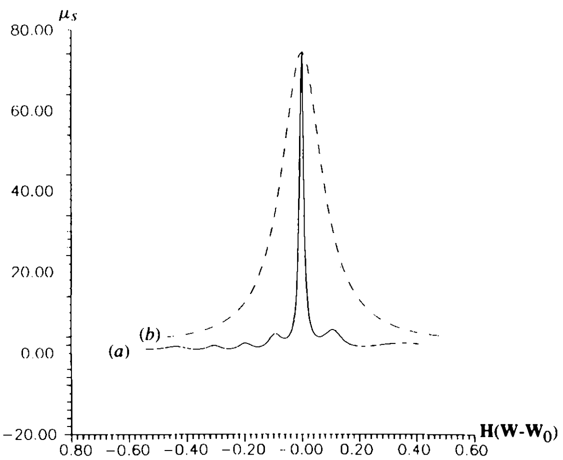


Fig. 5. (*a*) The very strong dependence of the diffractional suppression $\mu_s$ on the AW amplitude **W**. (*b*) The central part of (*a*) but the **W** scale is increased 10 times. $\mathbf{HW}_0 = 0.5878$, $T = 500\,\text{mm}$.

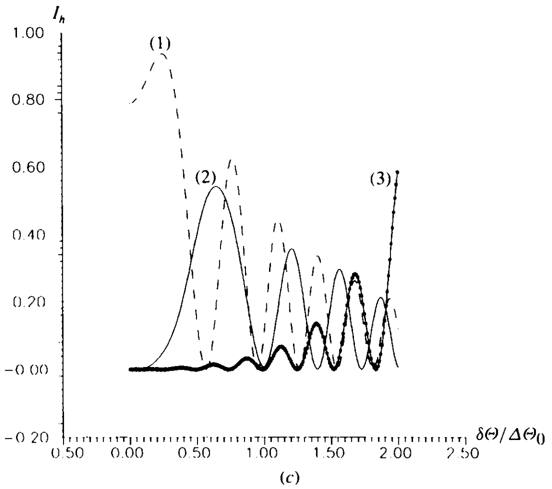


(*a*)

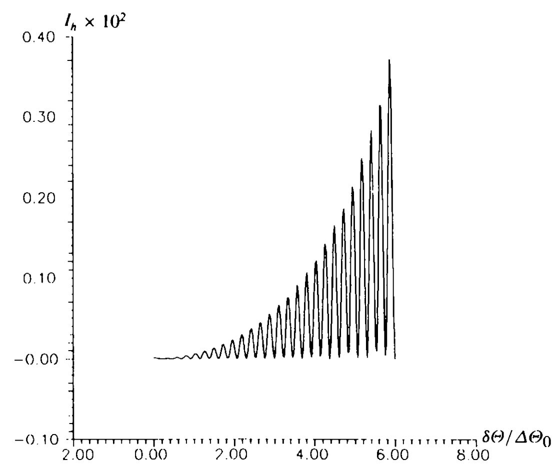


(*b*)

Fig. 6. The influence of the acoustic wavelength $\lambda_s$ on the suppression of the diffracted beam. $\tau = 115\,\mu\text{m}$, $T = 500\,\mu\text{m}$. (*a*) (1) $\mathbf{HW} = 0$; (2) $\mathbf{HW} = 1.477$, $\lambda_s = 500\,\mu\text{m}$; (3) $\mathbf{HW} = 0.587$, $\lambda_s = 50\,\mu\text{m}$. (*b*) $\mathbf{HW} = 0.6008$, $\lambda_s = 10\,\mu\text{m}$.

diffraction fringes in the diffracted or forward-scattering beams (26). Such experiments are realizable, probably using an Authier collimator and synchrotron-radiation impulses. A high-quality homogeneous AW is necessary for the success of such experiments.

We used boundary conditions (3). What can we expect when $T = (2n+1)\lambda_s/2$, $n = 1, 2, \ldots$? The suppression $\mu_s$ will not be as strong as before because this value is defined by the probability of scattering at the layer thickness $\lambda_s/2$, $P \simeq q^2$ [(15)] instead of $P \simeq q^4$ [(19)].

What can we say about $\mu_s$ dependence on the AW frequency? We have found $\mathbf{W}_0$ [(15)] using direct numerical solution of the Takagi–Taupin equations for the layer thickness $\lambda_s/2$ and momentum $q = 0$. The results of the numerical solution of the TT equations with AW amplitude $\mathbf{W} = \mathbf{W}_0$ and thickness of crystal $T = 500\,\mu\text{m}$ are presented in Fig. 6. Low-frequency AWs lead to a small suppression of the diffracted beam (Fig. 6*a*). Strong suppression of the diffracted beam is realized for the case of high-frequency ultrasound ($k_s \gg \Delta k_0$) when $J_0(4\mathbf{HW}) \simeq 0$, that is $\mathbf{HW} \simeq 0.6003$, $1.375, \ldots$ ($J_0$ is the Bessel function). High-frequency AWs strongly increase $\mu_s$ for our schematic model ($\tau = 115$, $T = 500\,\mu\text{m}$) with suppression of the diffracted-beam intensity; $\mu_s \simeq 5 \times 10^4$ (!) when $\lambda_s = 10\,\mu\text{m}$. The smoothing curve of the intensity of the diffracted beam (Fig. 6*b*) is well approximated as

$$I_h \simeq 2.8 \times 10^{-5} (\delta\Theta/\Delta\Theta_0)^{2.2} \qquad (28)$$

when $|\delta\Theta/\Delta\Theta_0| < 3$. Therefore, high-frequency ultrasonic AWs ($\lambda_s = 10\,\mu\text{m}$) and probably hypersound also lead to the strong and rapid suppression of the intensity of the diffracted beam outside the center of the diffraction pattern. This effect can be explained by the coefficients $C \simeq 1/k_s^{2-3}$ (18) when $\lambda_s < \tau$. Therefore, suppression of $\mu_s$ is large and exists in a wide angular interval of the incident beam. The crystal ($T = 500\,\mu\text{m}$) is effectively divided into many thin layers ($\lambda_s = 10\,\mu\text{m}$). The amplitude of scattering is very small in each of these thin layers.

It is likely that the rapid and deep suppression and oscillation of the intensity of the diffracted beam induced by ultrasound or hypersound could be used, in principle, for shielding electronic apparatus from the short powerful impulses of highly collimated monochromatic SR beams. The shielding from SR impulses is discussed in experiments with SR excitation of Mössbauer nuclei.

A considerable part of this work was done during the author's visit to the Nuclear Physics Institute (Rez, near Prague). I wish to express my appreciation to Professor P. Mikula, Dr P. Lukas and their colleagues for the hospitality. I am most grateful to Dr M. Vrana for many interesting discussions and to Dr L. Sedlakova, J. Saroun, P. Strunz, B. Michalkova and J. Vavra for their great technical assistance. I am especially grateful to L. Rusevich and Dr A. Muromtsev for the creation of the computer program.

### References

ENTIN, I. R. (1977). *Pis'ma Zh. Eksp. Teor. Fiz.* **26**, 392–395.
ENTIN, I. R. & PUCHKOVA, I. A. (1984). *Fiz. Tverd. Tela*, **26**, 3320–3324.
IOLIN, E. M. & ENTIN, I. R. (1983). *Zh. Eksp. Teor. Fiz.* **86**, 1692–1700.
IOLIN, E. M., RAITMAN, E. A., KUVALDIN, B. V. & ZOLOTOYABKO, E. V. (1988). *Zh. Eksp. Teor. Fiz.* **94**, 218–233.
IOLIN, E. M., ZOLOTOYABKO, E. V., RAITMAN, E. A., KUVALDIN, B. V. & GAVRILOV, V. N. (1986). *Zh. Eksp. Teor. Fiz.* **91**, 2132–2139.
KÖHLER, R., MÖHLING, W. & PEIBST, H. (1974). *Phys. Status Solidi B*, **61**, 173–180, 439–447.
KULDA, J., VRANA, M. & MUKULA, P. (1988). *Physica (Utrecht)*, B**151**, 122–129.
LANDAU, L. D. & LIFSHITZ, E. M. (1965). *Quatum Mechanics.* Oxford: Pergamon.
LUKAS, P. & KULDA, J. (1989). *Phys. Status Solidi B*, **6**, 41–48.
MIKULA, P., LUKAS, P. & KULDA, J. (1992). *Acta Cryst.* A**48**, 72–73.
SPENCER, W. J. & PEARMAN, G. T. (1970). *Adv. X-ray Anal.* **13**, 507–527.

*Acta Cryst.* (1995). A**51**, 902–909

# A Basic Factor of Dual Epitaxy: the Symmetry of Similarity of Zinc Blende Structure

BY LIN LI

*North China Research Institute of Electro-optics, Beijing* 100015, *People's Republic of China*

(*Received* 7 *November* 1994; *accepted* 19 *June* 1995)

## Abstract

The symmetry of the similarity of the surface step structure in zinc blende (sphalerite) type structures is investigated by studying the crystal planes that are parallel to the $[01\bar{1}]$ axis. The symmetry transformations of the similar plane pairs are derived. Plane sets (111) and (311) are the planes of symmetry. The similarity of the surface step structure exists among three sets of planes. The surface geometric characteristics of similar




ISSN 0108-7673 ©1995